Cryo-FIB for TEM investigation of soft matter and beam sensitive energy materials

Long, Daniel M.
Singh, Manish Kumar
Small, Kathryn
Watt, John Daniel

To be published in: Nanotechnology

DOI to publisher's version: 10.1088/1361-6528/ac92eb

Cryo-FIB for TEM Investigation of Soft Matter and Beam Sensitive Energy Materials

Daniel M. Long[1‖], Manish Kumar Singh[2], Kathryn Small[1] and John Watt[2*]

[1] Sandia National Laboratories, Albuquerque, NM 87123 USA

[2] Center for Integrated Nanotechnologies, Los Alamos National Laboratory, Los Alamos, NM 87545 USA

E-mail: watt@lanl.gov

‖ Current Address: Materials and Manufacturing Directorate, Air Force Research Laboratory, WPAFB, Dayton, OH 45433, USA. UES Inc., Beavercreek, OH 45432, USA.

Abstract

Primarily driven by structural biology, the rapid advances in cryogenic electron microscopy (cryo-EM) techniques are now being adopted and applied by materials scientists. Samples that inherently have electron transparency can be rapidly frozen (vitrified) in amorphous ice and imaged directly on a cryogenic transmission electron microscopy (cryo-TEM), however this is not the case for many important materials systems, which can consist of layered structures, embedded architectures, or be contained within a device. Cryogenic focused ion beam (cryo-FIB) lift-out procedures have recently been developed to extract intact regions and interfaces of interest, that can then be thinned to electron transparency and transferred to the cryo-TEM for characterization. Several detailed studies have been reported demonstrating the cryo-FIB lift-out procedure, however due to its relative infancy in materials science improvements are still required to ensure the technique becomes more accessible and routinely successful. Here, we review recent results on the preparation of cryo-TEM lamellae using cryo-FIB and show that the technique is broadly applicable to a range of soft matter and beam sensitive energy materials. We then present a tutorial that can guide the materials scientist through the cryo-FIB lift-out process, highlighting recent methodological advances that address the most common failure points of the technique, such as needle attachment, lift-out and transfer, and final thinning.

Key Words: cryogenic electron microscopy, cryogenic focused ion beam lift-out, cryo-FIB, low-Z energy materials, soft matter.

1. Introduction

Focused ion beam (FIB) milling in a scanning electron microscope (SEM) is one of the most powerful sample preparation methods for high-resolution characterization by transmission electron microscopy (TEM) due to its ability to pinpoint and extract specific regions and interfaces of interest.[1] FIB/SEM was primarily developed for use in the microelectronics industry to probe failure mechanisms of circuit components, and has further been exploited to prepare high quality TEM lamella for a variety of inorganic, organic, and bio-materials.[1] Some damage to the sample from the ion beam is always present even in supposedly beam-resistant materials, often manifesting as curtaining, redeposition of sputtered material, and surface and interface amorphization.[2] However, hydrated, low-Z, and soft materials that can be deformed thermally at low temperatures are prone to a greater a degree of beam damage which can potentially change the physical and chemical state of the sample through local heating, knock-on damage, radiolysis, and ion inclusion.[3, 4] For example, polymers are more susceptible to beam induced heating and local melting, but can also undergo chain scission and cross-linking.[5] Inorganic materials are generally more resilient (apart from zeolites), however dose rate and accumulated dose still need to be controlled to reduce the effects of beam damage.[6] To address these issues, techniques to mitigate beam-induced damage during TEM lamella preparation have been developed, such as performing the initial milling steps with a low-energy Ga^+ ion beam followed by final milling using low-energy Ar^+ ions, or increasing ion beam pitch (dwell overlap).[7-10] Cooling the stage and sample, and in some cases the entire instrument, to cryogenic temperatures to minimize FIB-induced damage is another promising approach and is having significant impact in a number of different areas including energy research, polymers, biological, and biomimetic materials.[11-13]

Much of the advances in cryogenic electron microscopy (cryo-EM) have been driven by the biological sciences. A target goal in biological imaging is to observe whole cells and their subcomponents as close to their native state as possible. Biological samples that are small enough to allow electron transparency, such as viruses and proteins, can be plunge frozen

(vitrified) and imaged in a cryogenic TEM (cryo-TEM) without further processing. If the specimens are larger, such as a cell, electron transparent sections must first be prepared that are on the order of tens to a few hundred nanometers thick. Traditionally, this has been performed by sample staining and fixation in a polymer resin, followed by sectioning with a diamond knife at room temperature (ultra-microtomy). However, this leads to alteration in cells and fine structure due to the external chemical used in fixation, dehydration, and epoxy embedding. Cryogenic ultramicrotomy eliminates the need for fixation and involves vitrification of the samples in a cryogen (typically liquid nitrogen, LN_2), often under the application of high pressure, and sectioning using a diamond knife that is maintained to cryogenic temperatures.[14-17] This method has been proven beneficial over fixation, however it is incredibly challenging.[18, 19] Moreover, the method still suffers from similar artifacts to room temperature microtomy preparation, including marks from the knife and mechanical deformation in the samples.[14, 17] Recently, much of the focus in biological research has shifted to cryogenically cooled focused ion beam (cryo-FIB) milling for TEM sample preparation, in order to produce a mostly artifact-free sample as close to its native state as possible. For example, Marko and coworkers have successfully prepared lamellae from frozen-hydrated *E. coli* cells using cryo-FIB milling for cryo-TEM imaging and tomography, without devitrification.[8] Preparation of frozen biological lamella using a cryo-FIB has been demonstrated by Rubino *et. al.* using a lift-out procedure similar to semiconductor methods, where a prepared lamella is removed using a cooled manipulator and a custom-built transfer station.[20] Preparing 'on-grid' lamellae eliminates the need for the challenging lift-out procedure, however this requires a sample (such as a growing cell) that can adhere to a support film on a TEM grid with a large contact area.[21]

Cryogenic electron microscopy (cryo-EM) for materials science can be considered a 'fast-follower' of the advances made in the technique for biology. However, it is now becoming apparent that materials science specific methods are required to fully exploit the impact of cryo-EM. Cryo-FIB is proving a powerful technique for creating electron transparent lamella from macroscopic beam sensitive and vitrified materials where dropcasting, plunge freezing, or microtoming are not applicable. Such cases are common in materials science where the region of interest may be buried within grown layers, bound to a monocrystalline wafer, or contained within a device. The use of cryo-FIB milling and cryo-TEM lamella preparation for materials science research can be classified into a few broad categories: 1) the characterization of hydrated

(or solvated) materials, in particular the imaging of liquid-solid interfaces, 2) the inert transfer of reactive low-Z materials and mitigation of beam damage 3) the preservation of sensitive layers and interfaces, and mitigation of artifact inclusion during milling and imaging. Cryo-FIB has been used to uncover the structure and chemistry of the electrode-electrolyte interface in Li-ion rechargeable batteries, which is a significant advance in understanding their structure-performance relationship.[22-24] Rapid vitrification of the liquid electrolyte preserved this critical interface in the near native state, which was then probed by cryo-STEM to characterize the structure and chemistry of the solid-electrolyte interphase (SEI), without beam-induced damage, or Li migration. Effective prevention of hydrogen incorporation in titanium-based alloys has been demonstrated at the sample preparation stage using cryo-FIB milling.[25] This prevented undesired hydrogen pick-up and hydride formation in commercially pure titanium and Ti-alloys which not only complicates microstructural characterization but also affects their mechanical properties. Sensitive 2D MoS_2 monolayers were preserved by using cryo-FIB during lamellae preparation of a remote epitaxy ZnO structure, to reveal a clean and abrupt interface that provided a novel platform for many body physics.[26]

This review and tutorial will introduce recent research enabled by cryo-FIB liftout and then guide the materials scientist through the cryo-FIB lift-out process and highlight the most common failure points of the method such as needle attachment, lift-out and transfer, and final thinning. We will detail unique process improvements for preparation of soft materials and beam-sensitive materials and highlight some of the key recent studies that have benefited from cryo-FIB sample preparation and cryo-TEM analysis.

2. TEM Lamellae of Energy and Soft Materials using Cryo-FIB

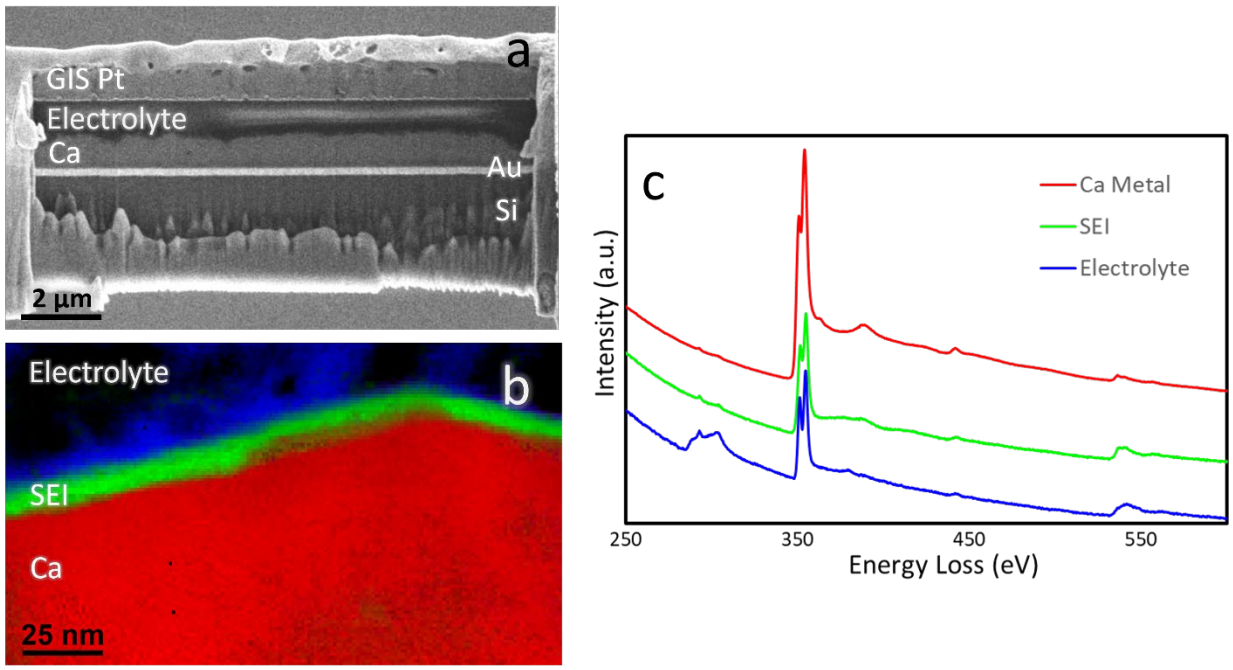

Figure 1. Cryo-EM analysis of a Ca metal anode battery cell. (a) Cryo-SEM imaging of the battery stack including the Si substrate, Au electrode, Ca metal anode, SEI, intact vitrified electrolyte, and GIS Pt cap. The vitrified electrolyte is electrically insulating which leads to charging artifacts in the image. (b) The principal component map from core loss EELS of the Ca metal and electrolyte interface indicates a thin and chemically unique SEI. (c) Core-loss EELS component spectra highlight the differences between the Ca metal and its terminating SEI.[27]

McClary and Long investigated the native solid electrolyte interphase (SEI) formed between a dense calcium metal anode and its electrolyte. Enabled by the SEI, rechargeable battery technologies based on Mg or Ca can deliver energy densities multiple times higher than current Li ion batteries without the safety issues facing Li metal anode batteries. The calcium metal anode battery half-cell was placed in secondary containers, removed from the glovebox, frozen slowly within the secondary containers, opened under cold N_2 gas or LN_2, and then brought into the cryo-FIB. Entering the workflow this way kept the reactive Ca metal, its interphase, and the electrolyte in their native states. Fastidious FIB milling and SEM imaging, such short dwell times and minimal imaging, and protective backside coatings of the lamella were essential to avoid destroying the sensitive vitrified electrolyte. Figure 1(a) shows the cryo-FIB lift-out in its final stages of thinning to electron transparency. In addition to the known components (Si substrate, the Au electrode, the Ca metal anode itself, the SEI not visible in figure 1(a), the electrolyte, and the gas injection system (GIS) Pt), charging (brightening) of the electrolyte is

visible due to the electrical resistance of the electrolyte. The principal component map (figure 1(b)) of the Ca metal (red), SEI (green), and electrolyte from core loss EELS mapping highlights the abruptness of the interface, the thinness of the SEI and its continuity. The principal components (Figure 1(c)) indicate the interphase is composed primarily of calcium oxide with borides and carborates intermixed. Although calcium oxide typically passivates further calcium transport due to its high migration energy barrier, the thinness of the film and its chemical heterogeneity likely allow for reversible and efficient calcium transport.

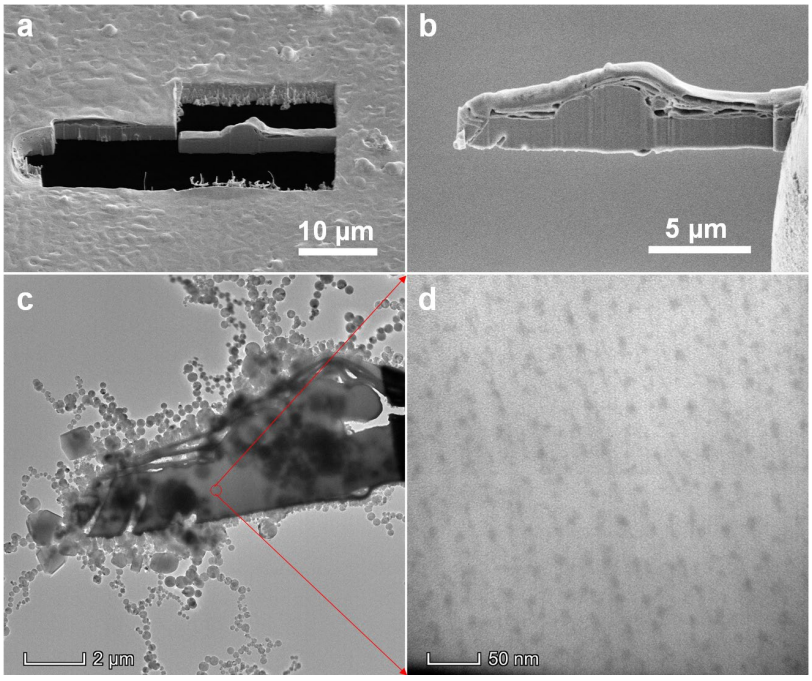

Figure 2. (a) Top-view cryo-SEM image of tungstate anion linked polypyrrole (TALPy) film cut by cryo-FIB. (b) Cross-sectional cryo-SEM image of TALPy fragment obtained by cryo-FIB. (c-d) Cryo-TEM images of TALPy fragment at low magnification (c) and high magnification (d), respectively.[28] Reprinted with permission from Reference 28.

Recently, Liu *et. al.* demonstrated a simple and scalable electrochemical deposition method for wafer-scale preparation of novel quasi-layered conductive organic-inorganic composite films with controllable size and thickness (figure 2). The quasi-layered composite film is denoted as tungstate anion linked polypyrrole (TALPy) and exhibits interesting capacitive properties with high volumetric capacitances and excellent charge-discharge stability in aqueous electrolytes. The internal structure of TALPy film was characterized using cryo-FIB and cryo-TEM (Figures 2(a) and 2(b)). Milling rates were incredibly fast with respect to silicon milled at room

temperature, and accelerating voltages that were too strong promoted delamination of the thin film from the substrate. Here, cryogenic conditions were used predominantly to mitigate beam damage; however, transfer was still need under cryogenic conditions to eliminate curling of the thin and flexible lamella. Ice particle contaminations were prevalent in the cryo-TEM sample (figure 2(c)), however there was sufficient clean area to observe the underlying microstructure. The dark spots in the grey matrix observed by cryo-TEM plausibly suggest tungstate aggregates, as shown in figure 2(d).

Nafion is an ion-conducting random copolymer used in many electrochemical applications as a solid electrolyte. Its common use is due to its excellent ion conductivity afforded by sulfonic acid groups, and good mechanical stability of a Teflon (tetrafluoroethylene) backbone, see figure 3(a). One of the most critical applications of Nafion is in proton exchange membrane (PEM) fuel cells, which are a viable candidate for clean-energy transportation, especially in a modernized heavy-duty vehicle fleet. Understanding how the membrane microstructure impacts ion transport is crucial for effective application and long-term stability of the material. Upon hydration Nafion swells to form hydrophilic water ‘clusters’, which determine ion transport based on their size and connectivity. Cryo-EM is the obvious choice for characterization since it operates while hydrated. Yamaguchi et. al. performed cryo-TEM on dispersed Nafion particles before and after heating.[29] Allen et. al. performed cryogenic electron tomography (cryo-ET) of an as-cast 100 nm frozen-hydrated Nafion membrane and identified a random channel-type interconnected network of hydrophilic domains.[30] Other studies have also imaged Nafion in the TEM, however again these were prepared specifically thin for TEM.[31-33] Nafion was also shown to degrade rapidly under electron beam irradiation, when performed at room temperature. However, casting conditions, film thickness, thermal history and degree of hydration all influence the resulting microstructure and ion transport properties so characterizing a sample closer to the operational state is vastly preferred. We performed cryo-FIB lift out on a frozen-hydrated Nafion sample, as shown in figure 3. Again, FIB milling occurs rapidly; however, cryogenic conditions reduce Ga^{+} beam sample interaction and mitigate curtaining. Despite some residual ice contamination occurring during the transfer, we were able to image the high-resolution microstructure of the material. Further, because final thinning and transfer were performed at cryogenic temperatures, we observed no curling or deformation of the electron transparent sample.

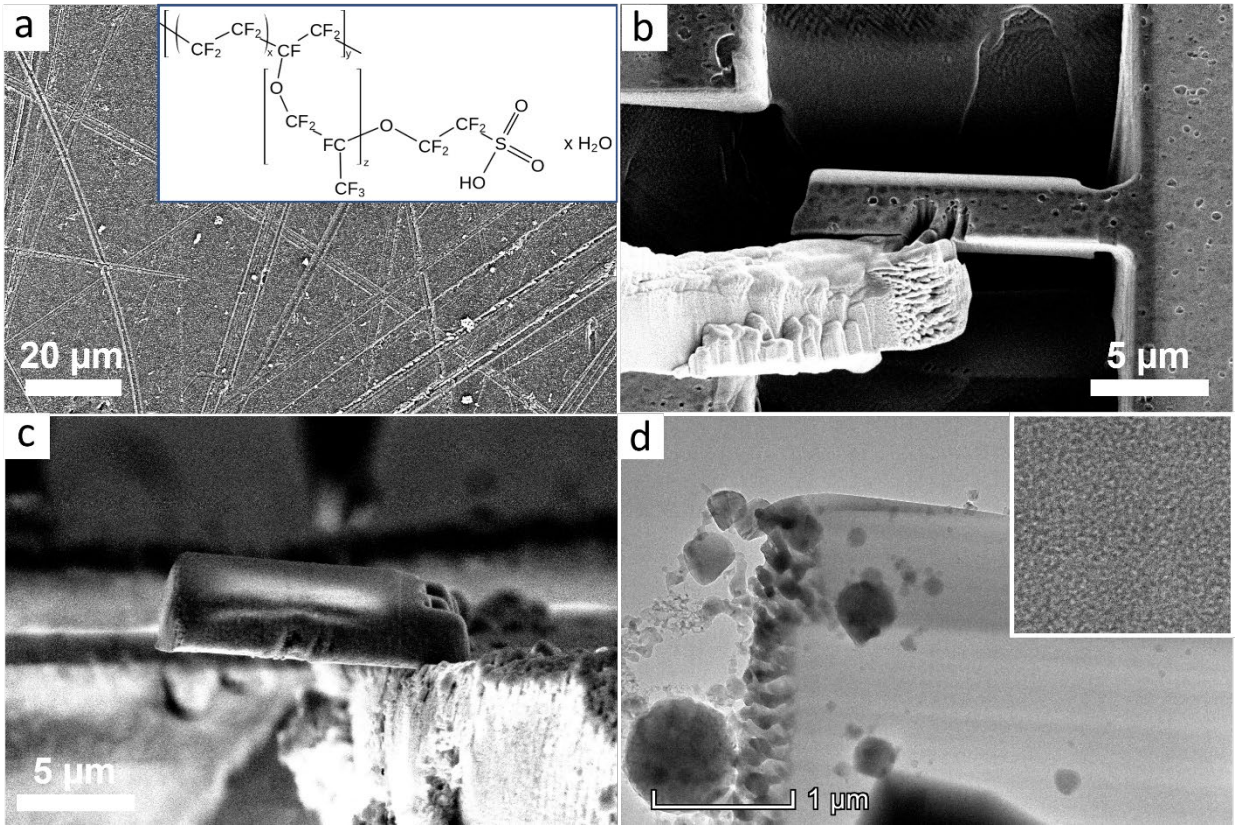

Figure 3. (a) Cryo-SEM image of a Nafion (inset) film; small amounts of ice contamination are present on the surface. (b) Fixing the lamella to the lift-out needle using the deposition-less attachment method. (c) Ion beam image of the transferred lamella waiting for thinning; charging indicates uncured protective Pt placed onto the backside of the lamella prior to lift-out. (d) Edge site of Nafion lamella, with ice contamination present and (inset) high magnification TEM image of Nafion, clearly showing the underlying hydrated microstructure.

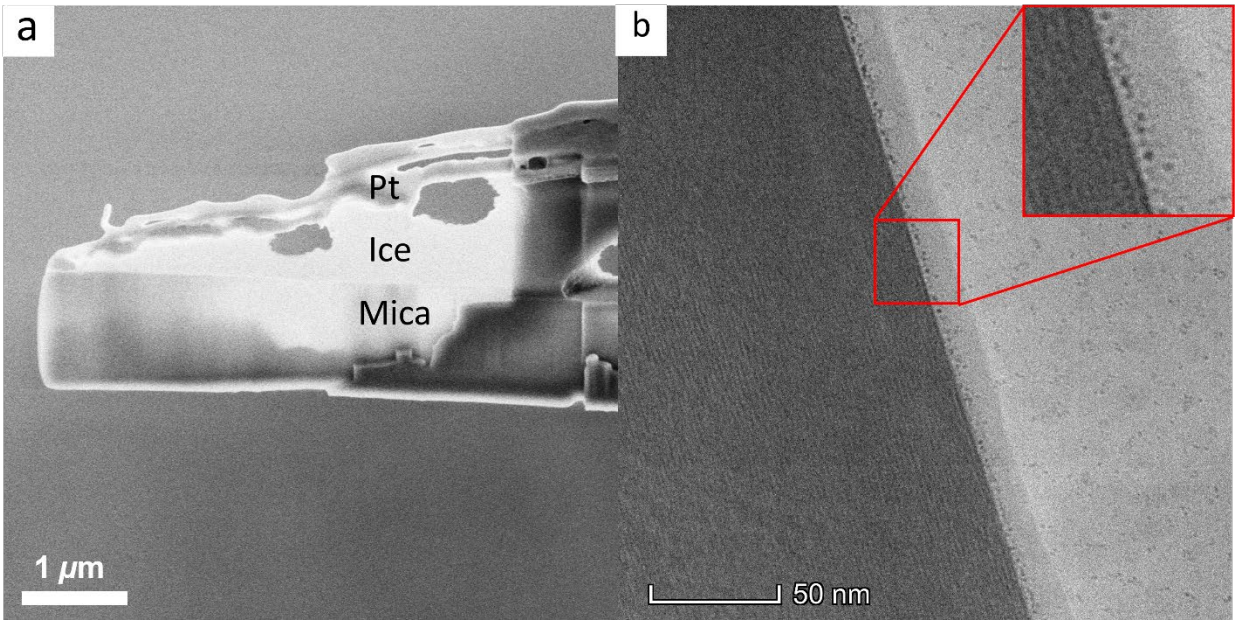

Figure 4. (a) Cryo-SEM of a TEM lamella prepared by cryo-FIB lift-out to image the Mica-NaAOT-water interface and (b) Cryo-TEM micrograph of the solid/liquid interface of muscovite mica with the 0.92 CMC Na-AOT solution containing 2.29 mM Na-AOT, 0.032 mM MgCl2 and 0.025 mM KCl. The sample was oriented so that the mica basal planes were parallel to the illumination for clear imaging of the interface. The inset shows a magnified view of the interface where AOT micelles can be seen.[34] Reproduced under open access.

Long *et al.* used cryo-FIB lift-out to prepare a lamella containing the interface between a muscovite mica basal plane and a solution of anionic surfactant dioctyl sodium sulfosuccinate (AOT or Aerosol-OT) for nanoscale cryo-TEM imaging (figure 4).[34] This study aimed to correlate the structure of the mineral/surfactant interface from cryo-TEM to that predicted from molecular dynamics simulations. Mica and its atomically smooth basal surfaces are a common substrate for fundamental research for applications involving subsurface energy extraction because of the prevalence of mica in earth's crust and mica's availability in research grade purity. Nanoscale imaging of the interface was possible with the cryo-FIB prepared sample while previous efforts using tomography of drop cast surfactant solutions on mica yielded poorer resolution. Cryo-FIB preparation proceeded as described above, except for the use exceptionally low beam currents to avoid 1) damage to the vitreous ice and 2) charging issues stemming from the sample being composed of two strong electrical insulators, mica, and ice. Cryo-TEM revealed that the AOT surfactant formed ~2 nm micelles which coalesced near the mica surface via a cation bridging mechanism.[34] Not only were the micelle dimensions the same as those

predicted by molecular dynamics simulations, but the small gap between the micelle and the mica surface were also corroborated.

3. Cryo-FIB Lift-Out Methods and Best Practices

The following section describes the general cryo-FIB lift-out procedure and best practices with a Thermo Fisher Scientific Scios 2 Dual Beam SEM/FIB retrofitted with Leica Microsystems cryogenic hardware and satellite cryogenic support and transfer equipment. In general, the cryo-FIB lift-out process follows the same principles of room temperature FIB lift-out, with a few critical exceptions; 1) the samples are vitrified or cooled to nearly liquid nitrogen temperatures before being analyzed, 2) the samples are kept cold during the lift-out and thinning process, and 3) traditional gas injection system (GIS) Pt welding cannot be used. These each pose their own unique challenges. Much of the fundamentals and process development of room temperature FIB lift-out can be found in the literature, along with some of the first methods papers for cryo-FIB.[8, 13, 20, 22, 25, 35-42] Here we build on these efforts to describe a generally applicable cryo-FIB lift-out procedure, with unique method developments, as well as broader best practices for the successful creation of cryogenic lamellae for cryo-TEM.

3.1 Preparing the Lab

Before any work can begin, the equipment must be prepared specifically for cryo-FIB lift-out. Having cryo-stages baked out and dry-LN_2 are the initial requirements. A hand-held LN_2 dewar should be dried overnight and filled from a dry hose on the lab dewar; as any frost accumulation on the hose can be inadvertently transferred to the FIB cooling dewars. Pernicious water content both in and on the equipment must be pumped, baked, or flushed out prior to use, including transfer equipment, gas venting lines, and the FIB chamber itself. An overnight pump of the vacuum equipment, a 5-minute gas line flush, and a 1-hour bake (dry) of tools is sufficient for removing the unwanted water. Any tools that come near a cooled sample should also be dried in a tool dryer (or with a hand-held hair dryer). In general, it is best to keep anything that has potential to condense water vapor or to accumulate ice baked and dry until immediately before it is needed. The cryogen, typically LN_2, that will meet the sample during loading and unloading should be as dry (low water content) as possible to minimize ice accumulation. This can be achieved by only using freshly dispensed LN_2 and baked-out hand dewars. LN_2 with visible ice

should never come into contact with the lamella because of the possibility of coating and obstructing the lamella with ice.

3.2 Preparing the grid/sample holder and liftout needle

Manipulating a standard Cu or Mo FIB half grid under a LN_2 bath is difficult, as its light weight can cause it to be lost in the turbulence if dropped. Further, it can be difficult to be precise with tweezers under the reduced visibility of boiling LN_2. A simple approach to improving success during manual manipulation of the grid is to adhere a Cu half grid to a more rigid Mo slot grid, as previously suggested by Zachman *et. al*.[13] The top of the slot grid can also be bent slightly backwards to ensure the post is visible when viewed from above while mounted upright, as sometimes the slot grids have some curvature that can make post visibility an issue, especially when tilted towards the ion beam (see Supplementary Video S2).

Regardless of the approach to connecting the lamella to the lift-out needle (redeposition vs condensing GIS material), the needle tip should be inspected prior to use to ensure it has suitable dimensions for attachment. For this approach, the lift-out needle shaft is rotated 52 degrees toward the ion beam and both the top and bottom of the needle are milled flat with a cleaning cross section until the needle is 1-2 μm wide (defining the width of the needle when rotated to its original position). Then the needle is rotated 90 degrees away from the ion beam (38 degrees past the neutral/original position) and cleaned on top and bottom until it is 3-4 μm (defining the side of the needle that will contact the lamella during lift-out). The needle is then rotated to the original position and possesses a 1-2 μm thick and 3-4 μm tall profile. The larger flat side allows for more contact with the sample while the thinner thickness allows for quick detachment once the sample is attached to the grid post.

3.3 Vitrification

Vitrifying and/or cooling the sample can be accomplished in a variety of ways including; 1) gradual cooling of the sample with the transfer shuttle (Leica VCT) or sample stage while under vacuum, 2) quick freezing in a liquid nitrogen bath (as can be done in the Leica VCM system) or slush nitrogen bath (as is typical of the of the Quorum PP3010), 3) vitrification by rapid plunging into liquid ethane with a Vitrobot (important for hydrated organics), or 4) by high pressure freezing (important for vitrifying larger organic samples). The exact cooling used for the material

system should be evaluated to confirm it does not induce artifacts. Once cooled care should be taken to not expose the sample to ambient air. Some workflows allow for manipulation under LN_2, or alternatively under a cold blanket of gaseous N_2, however often there is a step that requires transfer between cryogen containers. Protecting the sample with a cap and ensuring a quick and accurate transfer are the most prudent ways to avoid ice buildup.

3.4 Entering the cryo-EM workflow

In general, the workflow is both system and sample dependent. For example, a hydrated sample first requires rapid vitrification by plunge or high pressure freezing, followed by transfer to the cryo-FIB while avoiding ice contamination. Low-Z and reactive energy materials may follow the same pathway, such as if the native electrode-electrolyte interface is the region of interest, or they may be loaded under an inert atmosphere then cooled *in situ*, if only the low-Z metal structure is being investigated. Finally, a buried interface that is non-reactive, yet sensitive to the ion beam, can be loaded at room temperature and then cooled *in situ* before milling.

Materials that are only electron- or ion- beam sensitive, and which do not need strict atmospheric or temperature controls, can be loaded into the systems at room temperature and cooled with the equipment. Materials that require vitrification must be vitrified in equipment suitable for proper cooling rates. For example, aqueous solutions should be plunge frozen in cryogens suitable for rapid cooling and transferred cold to avoid crystallization. Systems that don't require rapid cooling, such as polymers, battery electrolytes, or whole battery stacks can be cooled at slower rates suitable to vitrify and freeze molecular mobility.[43] It should be noted that cooling systems too rapidly can lead to mechanical delamination of dissimilar phases which may lead to artifacts.[24] Finally, samples that require inert atmosphere transfers, such as reactive or toxic materials must be cooled while under an inert environment of a either vacuum or a mostly non-reactive gas such as Argon. Common approaches for these include placing the sample in a secondary container which is then submerged in LN_2 and opened once cold, or by transferring the samples into glovebox-interfacing cryo-equipment and then cooled with the tool.[44] Once inside the cryo-workflow and vitrified, a few nanometers of metal (e.g., Pt of Au) coating can be applied to dissipate charge that may accumulate on non-conductive samples (in the Leica Workflow this is done in the ACE600 with cryogenic stage attachment).

The Quorum PP 3010 and Leica cryo-FIB/SEM retrofitting systems, as well as the Thermo Fisher Scientific Aquilos dedicated cryo-FIB, make use of a small vacuum transfer vessel that connects to their respective preparation equipment and the FIB. The Leica cryo-FIB suite has independent and physically separated systems for loading (VCM), transfer (VCT 500), and sputtering/freeze fracturing (ACE 600), the Quorum system has the integrated loading station and sputter coater/freeze fracture equipment mounted onto the FIB, and the Aquilos has the loading station and sputter coater built into the chamber. The Leica system also has the additional option of interfacing its transfer vessel (VCT 500) directly with gloveboxes for environmentally sensitive work such as reactive or toxic materials. In full disclosure the authors have only used the Leica cryogenic workflow, and therefore make only qualitative comparisons between the systems

3.5 Complexities of working in a cryo-FIB

As noted earlier, cryo-FIB has additional layers of complexity on top of the typical FIB lift-out process. Samples may become more insulating at cryogenic temperatures, and while a few nanometers of sputter-coated metal can alleviate charging of insulating samples, thicker samples will still charge to some degree. The user will need to tune electron and ion beam parameters such as current, dose, energy, and dwell time to balance image clarity against sample stability. Low accelerating voltages and beam currents for both the electron and ion beams are recommended throughout the process to keep their interaction volumes to a minimum. If the equipment is not fully cooled, or if the beam dose and dwell times are too long, samples may undergo devitrification which will introduce artifacts. Small amounts of ice in LN_2 dewars attached to and cooling the FIB can act as nucleation points for boiling LN_2 which may translate vibration to the lift-out needle, and to a lesser extent the sample and stage, which will make attachment difficult and complicate final thinning. This is somewhat overcome with the use of cold N_2 gas as the thermal sink for the FIB/SEM stage.

Although most cryogenic vacuum systems have a cooled anti-contaminator (also referred to as a cold finger), the sample can still condense trace water vapor inside the chamber. If left cold for too long the ice build-up can obscure important contrast used for imaging and potentially lead to curtaining or incomplete milling. In some cryo-FIB systems the limited spatial mobility in the X,Y,Z, tilt, and rotation dimensions due to the cooling equipment may take away the ability to

utilize standard practices like rotating the sample 180 degrees to see the backside of the sample. Lastly, the use of a gas injected precursor for site-specific welding does not exist as the precursors typically used for FIB attachment, such as methylcyclopentadienyl trimethyl platinum, readily deposit over mm^2 areas across the sample. Therefore, other less straightforward methods must be used to attach the lamella to the lift-out needle and the TEM grid, which will be discussed below. We also recommend users do not use the 'hot-keys' and shortcuts they are familiar with in room temperature operation. Care must be taken to protect the cryo-stage at all costs, and the pace of work that comes from such a familiar type of operation can mistakenly lead to large stage movements, which can cause damage.

3.6 Locating the Region of Interest and Depositing a Protective Cap

Finding the region of interest for lift-out may be difficult in the case of samples with either laterally heterogeneous composition or buried interfaces. Energy dispersive X-ray spectroscopy (XEDS) or cryogenic correlative light and electron microscopy (cryo-CLEM) can be used in some cases to navigate to the ROI with thick vitreous overlayers or ice contamination.[42] Once the ROI is located its top surface must be protected for FIB lift-out. As mentioned above, a well-defined Pt cap over just the ROI is not possible. The Pt cap is instead deposited broadly and then cured by the ion beam over the ROI.

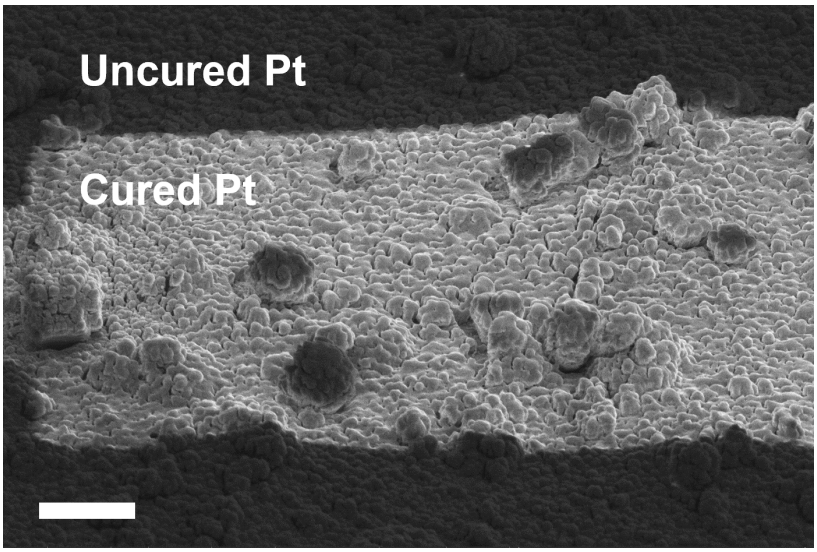

Figure 5. (a) Cryo-SEM image of cryogenic deposition of the protective Pt layer. The Pt is broadly distributed due to the thermal gradients associated with the cold sample, and then cured to a ROI post-deposition using the Ga^+ ion

beam. Also notice the lack of cured Pt within the 'shadow' of the features, due to the nature of initial deposition, which becomes less pronounced with decreasing surface roughness. Scale bar = 10 μm.

To do this, the gas injection system (GIS) needle is either not inserted to its typical room temperature lift-out position or it is retracted several mm, and its thermal setpoint is lowered to ambient temperature, down from the standard setting (45 ºC for the Scios 2). Both changes lower the precursor flux and allow for better control of the Pt layer thickness and reduce heat transfer to the sample. Next the GIS is opened, and the precursor is allowed to flow for a set amount of time which will depend on the microscope and the age of the Pt precursor. Approximate deposition times can be determined by observing the occlusion of surface features during deposition with the e^- beam. After deposition, the ion beam is scanned over the ROI until the condensed Pt precursor is 'cured'; the Ga^+ ion accelerating voltage should be set to 30 kV, with medium beam current (1.0 nA) to ensure complete curing (see Figure 5).[45] This curing process removes much of the organic precursor from the condensed layer and increases its density and conductivity. Uncured condensed precursor acts as an insulator, so it is recommended that a field of view larger than your ROI be cured before milling. We should also note that the delivery of the precursor is mostly direct on its path to the sample, so any texture of the surface can lead to shadowing and milling issues like curtaining or pore expansion from porosity in the Pt cap.

3.7 Trench milling

Removing the material around the ROI in cryo-FIB is largely like the room temperature process with minor differences. Two inward facing regular cross section patterns are typically used to mill around a ROI of a few micrometers thick. Local heating from the beam must be considered when deciding on the milling pattern type and its depth. Long dwell times typically used in cleaning cross section patterns or deeper regular cross section patterns can cause local heating that can lead to expansion, devitrification, melting, or sublimation of material. Rectangle patterns are a good alternative because beam dose is spread evenly across the patterned area in the time domain (beam is randomly rastered across the pattern), allowing more time for heat to flow away from the sample.

In general, we recommend keeping the ion beam accelerating voltage below 30 kV to minimize damage thickness and ion penetration into lower Z materials; 16 kV has proven successful with minimal loss of resolution. Trenches for solid-liquid interface TEM lamella are typically cut at

16 kV and a beam current of a few nA, and cleaning cross sections are generally performed at or below 500 pA.

3.8 *J*-Cut

The *J*-cut, or undercut, at cryogenic temperatures is also largely the same as it is at room temperature i.e., FIB milling is performed through two sides of the ROI, leaving a small amount of material connected on the third side. However, since cryo-samples are typically beam-sensitive materials, especially to the ion beam, we developed methods to protect the backside of the lamella (side imaged by the ion beam during *J*-cut) with a thin layer of material prior to performing the *J*-cut. This can be done in two ways, either 1) material from the trench surfaces is redeposited onto the sample, or 2) GIS Pt is condensed onto the sample. The first approach entails keeping the lamella parallel with the ion beam (52-degree stage tilt for Thermo Fisher Scios 2) and running a rectangle pattern in the bottom of the trench to redeposit material onto the lateral sides of the lamella. The second approach entails tilting the stage so that the backside of the lamella is visible to the GIS needle and then briefly flowing the precursor. The Pt on the backside of the lamella and the surrounding area can then be cured before proceeding, to ensure imaging stability. To demonstrate the effectiveness of protecting the lamella we carried out *stopping range of ions in matter* (SRIM) simulations of an unprotected polypropylene sample and a polypropylene material protected by a 100 nm thick layer of deposited precursor represented by 50% C / 50% Pt (figure 6). ~100 nm of deposited precursor or redeposited material takes less than a minute to accumulate on lamella surfaces. 30 kV Ga^+ ions were implanted at an angle of 52 degrees with respect to the side of the lamella to demonstrate the expected penetration to the polypropylene material during *J*-cut conditions.

In the unprotected polypropylene the Ga^+ ions, and the damage produced, penetrate at least 150 nm into the polypropylene material, while in the protected case the redeposited Pt/C layer protects the beam-sensitive surface entirely. While this SRIM simulation does not account for any complex beam interactions it does demonstrate the ease with which most beam damage can be stopped. In practice we have found that protective material that is thick enough to obscure the contrast of the ROI beneath it when imaging with secondary electrons is sufficient to eliminate damage incurred during the *J*-cut. If the stage cannot rotate 180 degrees due to the cryogenic stage being used one can estimate the appropriate protective layer thickness by first depositing

the protective layer on the front side until the secondary electron emission contrast is removed and then repeating the process on the backside.

If the ROI within the lamella is buried at a specific depth from the top surface, then the user can reveal the underlying sample stack by milling small cleaning patterns at the far sides of the now coated backside (these revealed regions will be removed during the *J*-cut). Once the backside is protected, the *J*-cut proceeds as normal. Care should be taken to not heat the sample with long dwell time patterns, especially once the j-cut is nearing completion, as the thermal contact is severely reduced.

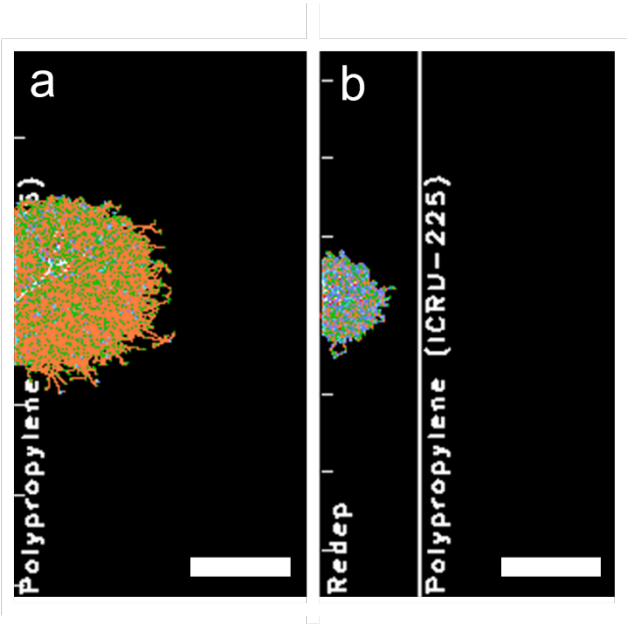

Figure 6. Stopping range of ions in matter (SRIM) simulation of (a) an unprotected polypropylene sample, compared to (b) a polypropylene material protected by a 100nm thick layer of deposited precursor represented by 50%C/50% Pt. Scale bars = 100 nm.

3.9 Needle Attachment and lift-out

Needle attachment and lift-out is where cryo-FIB diverges most significantly from room temperature operation. This step is highly dependent on the sample and on the experience and skill of the microscopist because small Pt welds are not possible at cryogenic temperatures. See Supplementary Video S1 for the complete procedure. Prior to being brought near the lamella the lift-out needle should be shaped as discussed above to simplify the rest of the lift-out process. Two approaches exist for connecting the lift-out needle to the sample, 1) use GIS chemistry or 2)

use local redeposited material.[42] In the first approach the needle is brought into contact with the lamella and then the GIS chemistry, either ice or Pt precursor is allowed to flow for a brief period of time. The GIS chemistry will create the material connection by coating the entire working area, including the ROI/needle interface.[38, 41] Once connected to the needle the remaining connection to the substrate is cut away and the lamella can be lifted out. This approach works well for making connections; however, the deposited GIS chemistries are insulators and may cause static electricity buildup which attracts the lamella back to the substrate from which it came during lifting the freed lamella. If Pt precursor is used it can be cured to reduce charging effects, but further ion beam exposure may damage the sample.

In the second approach the needle is brought into intimate contact with the lamella and thin, needle like, milling patterns are performed over the overlap (as shown in figure 7(a) and Supplementary Video S1). As the pattern mills through the lamella and into the needle, redeposited material builds up in the immediate area of the pattern, creating the physical connection for lift-out. Cleaning cross section patterns work well for attachment because they yield redeposition in a predictable amount and direction whereas the redeposition from a rectangle or circle pattern is less predictable and therefore not recommended. Once the first patterns are run and the milling depth is determined to be sufficient, the CCS patterns can be moved over fresh material away from the new connection and run again which will further guide sputtered material in the direction of the contact point. We recommend two ~ 200 x 1000 nm cleaning cross section patterns that begin centrally and progress outwards, followed by moving the patterning box outward to sputter fresh material (figure 7(a) and Supplementary Video S1). If done as described here and shown in figure 7 the microscopist will have a reliable connection for lift-out. Sharp focus of the ion beam is imperative here and imaging before and after all patterns is important to confirm progress. The remaining connection to the substrate is then cut and the sample lifted out.

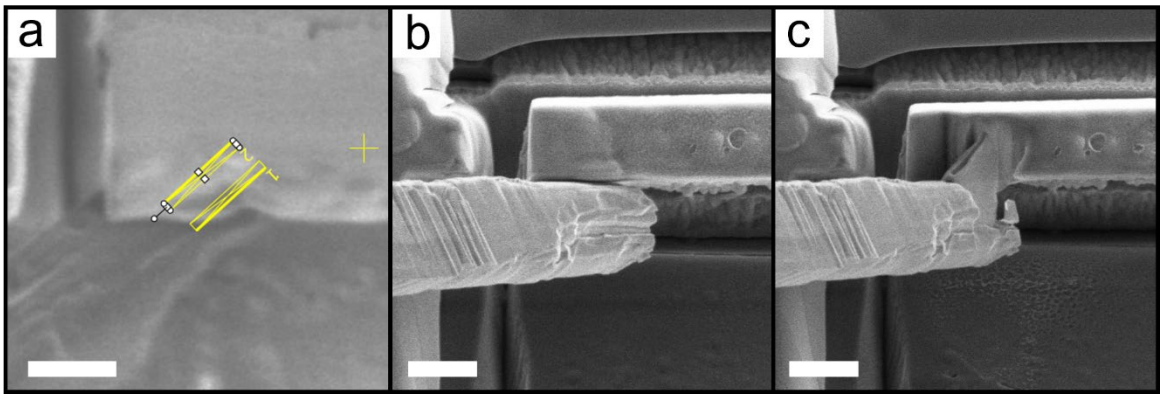

Figure 7. Setup and progression of a cryo-FIB needle attachment. (a)Two outward-facing thin cleaning cross section patterns are placed over the needle/lamella overlap, and the setup is imaged (b) before patterning and (c) after pattern completion. The area between the needle and the lamella is reliably connected with dense redeposited materials, i.e., the Pt/C capping layer and the tungsten needle. Scale bars = 2 μm.

3.10 Grid attachment and Final Thinning.

After the sample is lifted out of its substrate it is then transferred and attached to the TEM grid with either redeposited material as detailed above (recommended) or a coating of GIS material followed by cutting the connection to the lift-out needle (see Supplementary Video S2).[42] It is convenient to expedite needle detachment because the needle may have some thermal drift or vibration. Partially cutting the needle (figure 8(a), inset) close to the sample prior to touching the sample to the grid allows for quick detachment of the needle once the sample is fixed to the TEM grid. CCS patterns for redepositing material should start near the contact between the sample and grid and move away from there as shown, redepositing material in the direction of the contact point. The needle can be quickly cut free once the connection to the grid is made. Multiple points of contact to the grid should be made if using redeposited material (figure 8 and Supplementary Video S3) to stabilize the sample during final thinning and resist detachment during transport or storage in LN2.

Final thinning is largely sample dependent. In general, we recommend using beam energies and currents that are as low as reasonably acceptable. Pattern dwell times, especially when using cleaning cross section patterns, should be carefully chosen to limit local heating effects. The progress of the final thinning can be monitored with the secondary electron image contrast as shown in figure 8b; however, low-Z materials may appear bright at thicknesses too high for high

resolution TEM. It goes without saying that imaging the lamella should be kept to a minimum to limit dose to the sample.

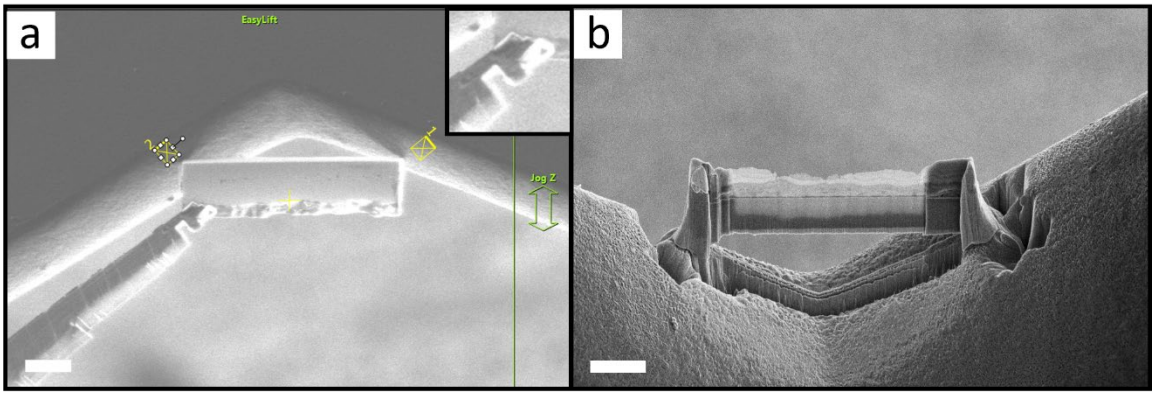

Figure 8. (a) Setup and progression of attachment of the TEM lamella to the FIB grid and (b) the final electron transparent region of interest. Scale bars = 5 μm.

4. Future Outlooks

Despite the clear progression of cryo-FIB for TEM sample preparation for materials science there are several aspects that inherently lag room temperature operation. Sample throughput is low, with one sample per day feasible for an experienced operator and assuming a successful experiment. This is due to slower procedures within the FIB, but also due to cryogenic transfer that requires specific cooling and baking out steps to be performed in order. Increasing throughput by custom designing stages that can hold multiple samples and half-grids, as well as automatic filling cryogen dewars would be useful. Automated software such as Thermo Fisher Scientific Auto Slice and View can be used to reduce operator time by making the initial rough cuts, however the full workflow cannot be used due to its reliance on Pt welding. As the popularity of cryo-FIB increases, the automation of deposition-less welding would have a significant impact. Rotation of the stage is a major limitation in cryo-FIB, as not all commercially available stages allowing for full freedom of movement. The Thermo Fisher Aquilos, for example, has full rotation due to the entire FIB being cooled, however it is very much focused on biological applications. Depending on the cooling mechanism, retrofitted cryogenic stages can allow for a good degree of movement, however full rotations are not always possible which limits the use of some common materials science characterization techniques. For example, cryo-EBSD maps and 3D tomographic reconstructions are difficult as the workflow

requires multiple 180° turns. Likewise, automated systems that rely on both e^- beam and ion beam fiducials, which require rotating between the two, are not possible with limited rotation.

The development of custom stages for cryogenic operation will increase thermal stability and yield more successful transfers and experiments. Take for example the 3D EBSD holder for performing 3D reconstructions on transferred chunk mills. Its long aspect ratio and small contact area to the sample does not offer great thermal transfer. Developing custom stages that contain some type of active cryogen (or thermal) transfer to the tip (and sample) could make the technique feasible under cryogenic conditions; especially due to the multiple milling and imaging steps (slices) needed for tomographic reconstruction. Further, custom cryogenic user profiles in the SEM/FIB software user interface that are stage specific would also help to protect the stage from erroneous movements, i.e., disabling the Nav-Cam to prevent the stage from mistakenly making the large movement towards it. Additionally, online user guides that interface with the SEM, as are already provided for room temperature operation, would allow for more successful cryo-FIB experiments.

5. Conclusion

Cryo-FIB allows for the extraction of regions and interfaces of interest that can then be characterized by high resolution TEM for structural and chemical analysis. Recent advances in cryo-FIB, primarily driven by structural biology, have been employed with good effect to answer important materials science questions. We show that his technique is broadly applicable in materials science, by forming high quality TEM lamellae of soft matter, hydrated, and beam sensitive energy materials. We then present a comprehensive tutorial to guide users new to cryo-FIB through the steps of lab and sample preparation, freezing and transfer, milling, lift-out and final thinning. In addition, we provide newly developed techniques to protect the lamella, connect the needle, and attach to the TEM grid. Our results will contribute to the more widespread use of cryo-FIB by increasing user confidence and the chances of a successful experiment. This will ensure that this powerful technique can more effectively facilitate advances in research areas where information about sensitive interfaces, hydrated structures, and beam sensitive materials are required.

Acknowledgements

This work was performed, in part, at the Center for Integrated Nanotechnologies, an Office of Science User Facility operated for the U.S. Department of Energy (DOE) Office of Science. Los Alamos National Laboratory, an affirmative action equal opportunity employer, is managed by Triad National Security, LLC for the U.S. Department of Energy's NNSA, under contract 89233218CNA000001. Sandia National Laboratories is a multimission laboratory managed and operated by National Technology & Engineering Solutions of Sandia, LLC, a wholly owned subsidiary of Honeywell International, Inc., for the U.S. DOE's National Nuclear Security Administration under contract DE-NA-0003525. The views expressed in the article do not necessarily represent the views of the U.S. DOE or the United States Government.

References

[1] Giannuzzi L A, Drown J L, Brown S R, Irwin R B and Stevie F A 1998 Applications of the FIB lift-out technique for TEM specimen preparation *Microsc. Res. Tech.* **41** 285-90

[2] Giannuzzi L A 2004 *Introduction to focused ion beams: instrumentation, theory, techniques and practice*: Springer Science & Business Media)

[3] Egerton R F 2012 Mechanisms of radiation damage in beam-sensitive specimens, for TEM accelerating voltages between 10 and 300 kV *Microsc. Res. Tech.* **75** 1550-6

[4] Watt J, Huber D L and Stewart P L 2019 Soft matter and nanomaterials characterization by cryogenic transmission electron microscopy *MRS Bull.* **44** 942-8

[5] Lee E H 1999 Ion-beam modification of polymeric materials - fundamental principles and applications *Nuclear Instruments & Methods in Physics Research Section B-Beam Interactions with Materials and Atoms* **151** 29-41

[6] Egerton R F 2019 Radiation damage to organic and inorganic specimens in the TEM *Micron* **119** 72-87

[7] Bals S, Tirry W, Geurts R, Yang Z and Schryvers D 2007 High-quality sample preparation by low kV FIB thinning for analytical TEM measurements *Microsc. Microanal.* **13** 80-6

[8] Marko M, Hsieh C, Schalek R, Frank J and Mannella C 2007 Focused-ion-beam thinning of frozen-hydrated biological specimens for cryo-electron microscopy *Nat Methods* **4** 215-7

[9] Zhong X L, Haigh S J, Zhou X and Withers P J 2020 An in-situ method for protecting internal cracks/pores from ion beam damage and reducing curtaining for TEM sample preparation using FIB *Ultramicroscopy* **219** 113135

[10] Bassim N D, De Gregorio B T, Kilcoyne A L D, Scott K, Chou T, Wirick S, Cody G and Stroud R M 2012 Minimizing damage during FIB sample preparation of soft materials *Journal of Microscopy* **245** 288-301

[11] Obst M, Gasser P, Mavrocordatos D and Dittrich M 2005 TEM-specimen preparation of cell/mineral interfaces by Focused Ion Beam milling *Am. Mineral.* **90** 1270-7

[12] Weber P K, Graham G A, Teslich N E, Chan W M, Ghosal S, Leighton T J and Wheeler K E 2010 NanoSIMS imaging of Bacillus spores sectioned by focused ion beam *J Microsc* **238** 189-99

[13] Zachman M J, Asenath-Smith E, Estroff L A and Kourkoutis L F 2016 Site-Specific Preparation of Intact Solid-Liquid Interfaces by Label-Free In Situ Localization and Cryo-Focused Ion Beam Lift-Out *Microsc. Microanal.* **22** 1338-49

[14] Al-Amoudi A, Studer D and Dubochet J 2005 Cutting artefacts and cutting process in vitreous sections for cryo-electron microscopy *J Struct Biol* **150** 109-21

[15] Al-Amoudi A, Dubochet J, Gnaegi H, Luthi W and Studer D 2003 An oscillating cryo-knife reduces cutting-induced deformation of vitreous ultrathin sections *J Microsc* **212** 26-33

[16] Hsieh C E, Marko M, Frank J and Mannella C A 2002 Electron tomographic analysis of frozen-hydrated tissue sections *J Struct Biol* **138** 63-73

[17] Zhang P, Bos E, Heymann J, Gnaegi H, Kessel M, Peters P J and Subramaniam S 2004 Direct visualization of receptor arrays in frozen-hydrated sections and plunge-frozen specimens of E. coli engineered to overproduce the chemotaxis receptor Tsr *J Microsc* **216** 76-83

[18] Al-Amoudi A, Diez D C, Betts M J and Frangakis A S 2007 The molecular architecture of cadherins in native epidermal desmosomes *Nature* **450** 832-7

[19] Pierson J, Fernandez J J, Bos E, Amini S, Gnaegi H, Vos M, Bel B, Adolfsen F, Carrascosa J L and Peters P J 2010 Improving the technique of vitreous cryo-sectioning for cryo-electron tomography: electrostatic charging for section attachment and implementation of an anti-contamination glove box *J Struct Biol* **169** 219-25

[20] Rubino S, Akhtar S, Melin P, Searle A, Spellward P and Leifer K 2012 A site-specific focused-ion-beam lift-out method for cryo Transmission Electron Microscopy *J Struct Biol* **180** 572-6

[21] Wagner F R, Watanabe R, Schampers R, Singh D, Persoon H, Schaffer M, Fruhstorfer P, Plitzko J and Villa E 2020 Preparing samples from whole cells using focused-ion-beam milling for cryo-electron tomography *Nat Protoc* **15** 2041-70

[22] Zachman M J, Tu Z, Choudhury S, Archer L A and Kourkoutis L F 2018 Cryo-STEM mapping of solid-liquid interfaces and dendrites in lithium-metal batteries *Nature* **560** 345-9

[23] Jungjohann K L, Gannon R N, Goriparti S, Randolph S J, Merrill L C, Johnson D C, Zavadil K R, Harris S J and Harrison K L 2021 Cryogenic Laser Ablation Reveals Short-Circuit Mechanism in Lithium Metal Batteries *Acs Energy Letters* **6** 2138-44

[24] Harrison K L, Merrill L C, Long D M, Randolph S J, Goriparti S, Christian J, Warren B, Roberts S A, Harris S J, Perry D L and Jungjohann K L 2021 Cryogenic electron microscopy reveals that applied pressure promotes short circuits in Li batteries *iScience* **24** 103394

[25] Chang Y, Lu W, Guenole J, Stephenson L T, Szczpaniak A, Kontis P, Ackerman A K, Dear F F, Mouton I, Zhong X, Zhang S, Dye D, Liebscher C H, Ponge D, Korte-Kerzel S, Raabe D and Gault B 2019 Ti and its alloys as examples of cryogenic focused ion beam milling of environmentally-sensitive materials *Nat Commun* **10** 942

[26] Kim Y, Watt J, Ma X, Ahmed T, Kim S, Kang K, Luk T S, Hong Y J and Yoo J 2022 Fabrication of a Microcavity Prepared by Remote Epitaxy over Monolayer Molybdenum Disulfide *ACS Nano* **16** 2399-406

[27] McClary S A, Long D M, Sanz-Matias A, Kotula P G, Prendergast D, Jungjohann K L and Zavadil K R 2022 A Heterogeneous Oxide Enables Reversible Calcium Electrodeposition for a Calcium Battery *ACS Energy Letters* **7** 2792-800

[28] Liu H B, Liang J X, Watt J, Tilley R D, Amal R and Wang D W 2021 Wafer-scale quasi-layered tungstate-doped polypyrrole film with high volumetric capacitance *Nano Research*

[29] Yamaguchi M, Terao T, Ohira A, Hasegawa N and Shinohara K 2019 Size and shape of Nafion particles in water after high-temperature treatment *Journal of Polymer Science Part B-Polymer Physics* **57** 813-8

[30] Allen F I, Comolli L R, Kusoglu A, Modestino M A, Minor A M and Weber A Z 2015 Morphology of Hydrated As-Cast Nafion Revealed through Cryo Electron Tomography *ACS Macro Lett* **4** 1-5

[31] Xue T, Trent J S and Osseoasare K 1989 Characterization of Nafion Membranes by Transmission Electron-Microscopy *Journal of Membrane Science* **45** 261-71

[32] Yakovlev S, Balsara N P and Downing K H 2013 Insights on the study of nafion nanoscale morphology by transmission electron microscopy *Membranes (Basel)* **3** 424-39

[33] Peltonen A, Etula J, Seitsonen J, Engelhardt P and Laurila T 2021 Three-Dimensional Fine Structure of Nanometer-Scale Nafion Thin Films *Acs Applied Polymer Materials* **3** 1078-86

[34] Long D M, Greathouse J A, Xu G P and Jungjohann K L 2022 Molecular Dynamics Simulation and Cryo-Electron Microscopy Investigation of AOT Surfactant Structure at the Hydrated Mica Surface *Minerals* **12**

[35] Giannuzzi L A and Stevie F A 2005 *Introduction to Focused Ion Beams* (Boston, MA: Springer)

[36] Strunk K M, Wang K, Ke D, Gray J L and Zhang P 2012 Thinning of large mammalian cells for cryo-TEM characterization by cryo-FIB milling *J Microsc* **247** 220-7

[37] Mahamid J, Schampers R, Persoon H, Hyman A A, Baumeister W and Plitzko J M 2015 A focused ion beam milling and lift-out approach for site-specific preparation of frozen-hydrated lamellas from multicellular organisms *J Struct Biol* **192** 262-9

[38] Parmenter C D, Fay M W, Hartfield C and Eltaher H M 2016 Making the practically impossible "Merely difficult"--Cryogenic FIB lift-out for "Damage free" soft matter imaging *Microsc. Res. Tech.* **79** 298-303

[39] He J, Hsieh C, Wu Y, Schmelzer T, Wang P, Lin Y, Marko M and Sui H 2017 Cryo-FIB specimen preparation for use in a cartridge-type cryo-TEM *J Struct Biol* **199** 114-9

[40] Schreiber D K, Perea D E, Ryan J V, Evans J E and Vienna J D 2018 A method for site-specific and cryogenic specimen fabrication of liquid/solid interfaces for atom probe tomography *Ultramicroscopy* **194** 89-99

[41] Parmenter C D and Nizamudeen Z A 2021 Cryo-FIB-lift-out: practically impossible to practical reality *J Microsc* **281** 157-74

[42] Klumpe S, Kuba J, Schioetz O H, Erdmann P S, Rigort A and Plitzko J M 2022 Recent Advances in Gas Injection System-Free Cryo-FIB Lift-Out Transfer for Cryo-Electron Tomography of Multicellular Organisms and Tissues *Microscopy Today* **30** 42-7

[43] Monnier X and Cangialosi D 2019 Effect of molecular weight on vitrification kinetics and molecular mobility of a polymer glass confined at the microscale *Thermochim. Acta* **677** 60-6

[44] Li Y, Li Y, Pei A, Yan K, Sun Y, Wu C L, Joubert L M, Chin R, Koh A L, Yu Y, Perrino J, Butz B, Chu S and Cui Y 2017 Atomic structure of sensitive battery materials and interfaces revealed by cryo-electron microscopy *Science* **358** 506-10

[45] Salvador-Porroche A, Sangiao S, Philipp P, Cea P and Teresa J M 2020 Optimization of Pt-C Deposits by Cryo-FIBID: Substantial Growth Rate Increase and Quasi-Metallic Behaviour *Nanomaterials (Basel)* **10** 1906